Self-Scheduled Control of a Gyroscope

Julian Theis [*] Christian Radisch [**] Herbert Werner [*]

[*] *Institute of Control Systems, Hamburg University of Technology,
Hamburg, Germany (e-mail: julian.theis@tuhh.de, h.werner@tuhh.de).*
[**] *Institute of Mechanics and Ocean Engineering, Hamburg University
of Technology, Hamburg, Germany (e-mail: christian.radisch@tuhh.de)*

Abstract: A classical mixed sensitivity minimization approach and a model matching formulation are compared with the goal to design a linear parameter-varying augmented state feedback control law for a laboratory-scale control moment gyroscope. Dynamic weighting filters are used to impose integral action and roll-off on the controller. Consequently, measurement noise is effectively suppressed and steady state accuracy is guaranteed even in the presence of input disturbances. Both designs are validated in real-time experiments and compared to a previous design that uses static weights. With the new designs, control effort is reduced while transient performance is maintained and tracking accuracy, as well as disturbance attenuation, is improved.

Keywords: Linear parameter-varying systems, Robust control applications, Robust controller synthesis, Gyroscopes, Mixed sensitivity problem, Multivariable control systems

1. INTRODUCTION

Control moment gyroscopes are inherently coupled nonlinear plants and therefore difficult to control by standard linear design methods. They are used, e. g., in attitude control of spacecraft and stability augmentation of ships. In this paper, a laboratory-scale control moment gyroscope, the ECP model 750 [1], is used as a testbed for linear parameter-varying (LPV) gain scheduled controller design.

Recently, first successful experimental validation of an LPV control strategy for the ECP 750 has been reported in Abbas et al. (2013, 2014), demonstrating that the plant can be stabilized in a wide operating range. Still, some specifications with practical relevance, such as input disturbance attenuation, were not considered and steady state accuracy relied on a static prefilter.

To address these issues, an LPV state feedback controller augmented with dynamic weighting filters is designed in this paper. The dynamic weights allow to guarantee steady state accuracy through integral control, which also results in effective rejection of input disturbances. Further, a roll-off is included in the controller to reduce sensitivity to measurement noise. Two different design approaches are pursued: a classical S/KS mixed sensitivity minimization and a model matching formulation. The new designs are experimentally validated and the results are compared to the ones reported by Abbas et al. (2014).

The paper is structured as follows: Section 2 describes the plant and the LPV model used in synthesis, detailing the predominant dynamic effects. Section 3 briefly reviews LPV synthesis machinery and the different design approaches are discussed in Section 4. Section 5 presents an experimental comparison of the different controllers and draws conclusions.

---

[1] See `www.ecpsystems.com/controls_ctrlgyro.htm` for details.

2. PLANT DESCRIPTION

The control moment gyroscope is a flywheel suspended in a gimbal mounting and is modeled with Neweul-M[2] (Kurz et al. (2010)) as a four-degree-of-freedom multibody system. The system is in chain structure, i. e., without kinematic loops. Each body is linked to the previous body by a rotational joint perpendicular to the last joint axis. A kinematic model is depicted in Fig. 1.
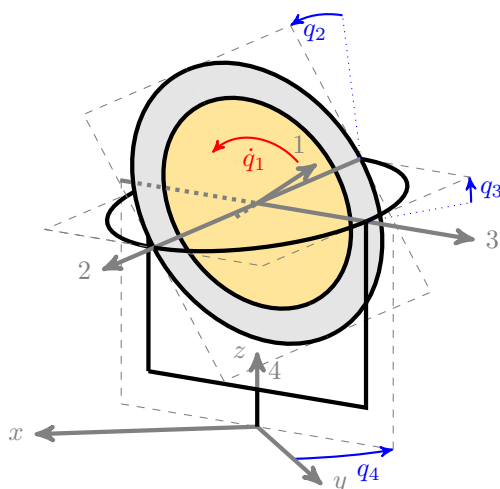

Fig. 1. Kinematics of the control moment gyroscope

The nonlinear equations of motion in minimal form are

$$M(q)\,\ddot{q} + k(q,\dot{q}) = f(\dot{q}) + \begin{bmatrix} I \\ 0 \end{bmatrix} \begin{bmatrix} T_1 \\ T_2 \end{bmatrix}, \qquad (1)$$

where $q = [q_1\ q_2\ q_3\ q_4]^T$, M is the mass matrix, k the vector of generalized nondissipative forces including gyroscopic terms, and f is the vector of generalized dissipative forces. The inputs T_1 and T_2 represent torques applied by

electric motors at axis 1 and 2, respectively. The controlled outputs considered in this paper are the unactuated angles $y = [\, q_3 \;\; q_4 \,]^T$.

2.1 Linear Parameter-Varying Model

For synthesis purposes, a simplified model with state $x = [q_3 \;\; q_4 \;\; \dot{q}_2 \;\; \dot{q}_3 \;\; \dot{q}_4]^T$ is used. It was introduced and validated in Abbas et al. (2014) and is based on linearization about a moving operating point $\rho(t) = [\dot{q}_1(t) \;\; q_2(t) \;\; q_3(t)]^T$. Note that this is not an equivalent formulation of the nonlinear system (1), but rather represents a continuous family of Jacobian linearizations.

The parametrization of a nonlinear system in terms of a varying operating point is a classical approach for gain scheduling control, see e.g. Rugh and Shamma (2000). Formally, the operating point is defined by the time-varying parameter vector $\rho \colon \mathbb{R} \to \mathcal{P}$ with a compact set $\mathcal{P} \subset \mathbb{R}^{n_\rho}$ of admissible parameter trajectories. A parameter-dependent state space representation is then

$$\dot{x} = A(\rho(t))\, x + B(\rho(t))\, u \tag{2a}$$
$$y = C(\rho(t))\, x + D(\rho(t))\, u \tag{2b}$$

with the continuous matrix functions $A \colon \mathcal{P} \to \mathbb{R}^{n_x \times n_x}$, $B \colon \mathcal{P} \to \mathbb{R}^{n_x \times n_u}$, $C \colon \mathcal{P} \to \mathbb{R}^{n_y \times n_x}$, $D \colon \mathcal{P} \to \mathbb{R}^{n_y \times n_u}$ and the state $x \colon \mathbb{R} \to \mathbb{R}^{n_x}$, input $u \colon \mathbb{R} \to \mathbb{R}^{n_u}$ and output $y \colon \mathbb{R} \to \mathbb{R}^{n_y}$ and with the scheduling signal ρ.

Since the operating point, and thus the parameter vector, cannot change arbitrarily fast, rates of change $\dot{\rho} \colon \mathbb{R} \to \mathcal{V}$ in the parameters are defined to lie within the polyhedron $\mathcal{V} = \{v \in \mathbb{R}^{n_\rho} \mid |v_i| \le \nu_i, \quad i = 1, \ldots, n_\rho\}$. Further, as the trajectories are not known a priori, the parameter space $\mathcal{P} \times \mathcal{V}$ is represented by auxiliary variables $p \in \mathcal{P}$ and $v \in \mathcal{V}$. For brevity, the explicit dependence on time and parameters is dropped from this point on.

2.2 Predominant Dynamic Variations

The distribution of control inputs to the controlled outputs varies strongly and depends mainly on the angle q_2. For $q_2 = 0$, the system is decoupled. Applying torque to axis 1 then produces a reactive torque resulting in a negative motion around axis 3. Torque applied to axis 2, on the other hand, results in precession and rotates the device around axis 4. This however also changes q_2, which inevitably introduces cross couplings. The effect is illustrated in Fig. 2, where it is shown that the directions of the cross couplings depend on the sign of q_2. For $q_2 = \pm 90°$, the allocation of inputs and outputs completely swaps. The system is thus only diagonal dominant in the vicinity of $q_2 = 0$.

The angle q_3 also strongly influences the dynamics. Fig. 3 depicts the input-output pole zero map from the second input to q_4 for $q_2 = 0$ and different frozen values of q_3. It shows that for positive q_3, there is non-minimum phase behavior which becomes more dominant, i.e., slower, with more inclination and for $q_3 = \pm 90°$ results in a zero at the origin. For $q_3 = 0°$, the zero is located at infinity, leading to a change in the relative degree of the system. The dominant pole pair further approaches the origin for $q_3 \to \pm 90°$, indicating that the system bandwidth decreases while damping increases.
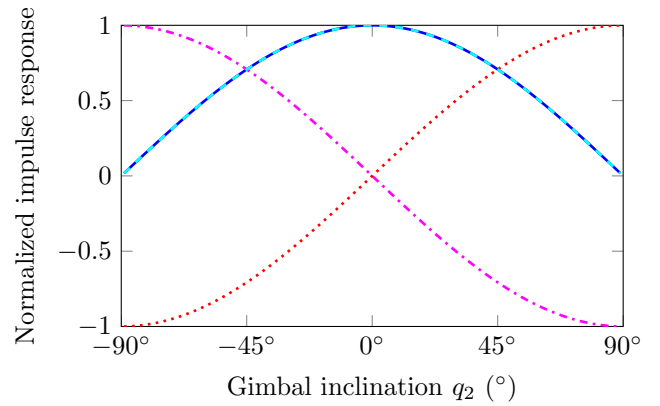
Fig. 2. Normalized impulse response gain for different values of $q_2 \in [-90°, 90°]$: $T_1 \to q_3$ (——) and $T_1 \to q_4$ (—·—·—); $T_2 \to q_3$ (·······) and $T_2 \to q_4$ (– – –)
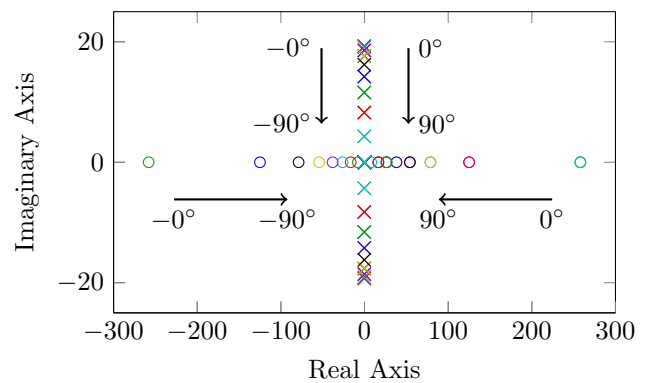
Fig. 3. Input-output pole-zero map $T_2 \to q_4$ for different values of $q_3 \in [-90°, 90°]$

The angular velocity $\dot{q}_1$ of the flywheel also changes the location of the dominant pole pair: larger velocities increase the resonant frequency, lower velocities decrease it. Damping is only marginally affected by variations in $\dot{q}_1$.

3. LPV GAIN SCHEDULING

The controller synthesis procedure employed in this paper was developed in Wu (1995); Wu et al. (1996). It specifies performance in terms of the induced $\mathcal{L}_2$-norm of a generalized plant.

A generalized LPV plant P is said to have an induced $\mathcal{L}_2$-norm $\|P\|$ if there exists a constant $\gamma > 0$ such that for all $z = P\, w$, $w \in \mathcal{L}_2$, and $(p, v) \in \mathcal{P} \times \mathcal{V}$

$$\|z\|_2 \le \gamma \|w\|_2, \quad \|z\|_2 = \sqrt{\int_0^\infty z^T(\tau)\, z(\tau)\, \mathrm{d}\tau}. \tag{3}$$

A guaranteed induced $\mathcal{L}_2$-norm and stability of a closed-loop system can be achieved by state feedback control with the following theorem.

Theorem 1. (Wu (1995)). Let a compact set $\mathcal{P} \times \mathcal{V}$, a performance specification $\gamma > 0$ and a generalized LPV plant of the form

$$\begin{bmatrix} \dot{x} \\ z_1 \\ z_2 \end{bmatrix} = \left[\begin{array}{c|cc} A & B_1 & B_2 \\ \hline C_{11} & 0 & 0 \\ C_{12} & 0 & I \end{array} \right] \begin{bmatrix} x \\ w \\ u \end{bmatrix} \tag{4}$$

be given. Further, let $R : \mathcal{P} \to \mathbb{R}^{n_x \times n_x}$ be a continuously differentiable symmetric matrix function such that for all $(p, v) \in \mathcal{P} \times \mathcal{V}$

$$R \succ 0 , \quad (5a)$$

$$\begin{bmatrix} \Psi & R\,C_{11}^T & \gamma^{-1}\,B_1 \\ C_{11}\,R & -I & 0 \\ \gamma^{-1}\,B_1^T & 0 & -I \end{bmatrix} \prec 0 , \quad (5b)$$

with $\Psi = R\,(A - B_2\,C_{12})^T + (A - B_2\,C_{12})\,R$

$$-B_2\,B_2^T - \sum_{i=1}^{n_\rho} \frac{\partial R}{\partial p_i}\,v_i .$$

The state feedback control law

$$u = -\left(B_2^T\,R^{-1} + C_{12}\right)x \quad (6)$$

renders the closed-loop system asymptotically stable with an induced $\mathcal{L}_2$-norm less than γ.

Since the linear matrix inequality (LMI) constraints (5) are infinite dimensional due to the functional dependence on the scheduling parameter p, it is proposed in Wu (1995) to grid the parameter space. The constraints are then only enforced on a finite dimensional set $\{p_k\} \in \mathcal{P}$. Consequently, sufficiency of the conditions in between grid points is lost but due to continuity, the solution remains valid for a sufficiently dense grid.

Further, the arbitrary dependence of the Lyapunov matrix R on p needs to be restricted to arrive at a tractable formulation. Selecting basis functions g_i for the Lyapunov matrix

$$R(p) = \sum_{i=1}^{n_R} R_i\,g_i(p) \quad (7)$$

then leads to the semidefinite program

$$\min_{\gamma, \{R_i\}_1^{n_R}} \gamma \text{ such that}$$
$$\text{LMI (5) holds } \forall (p, v) \in \{p_k\} \times \text{vert}\,(\mathcal{V}) \quad (8)$$

where vert$(\mathcal{V})$ denotes the vertices of the polyhedron $\mathcal{V}$.

4. MIXED SENSITIVITY DESIGN

Mixed sensitivity minimization is a very versatile tool for control design, see e.g. Zhou et al. (1995); Skogestad and Postlethwaite (2005). Its general two-block representation is

$$\min_K \left\| \begin{bmatrix} W_1\,S \\ W_2\,K\,S \end{bmatrix} W_3 \right\| , \quad (9)$$

where $S = (I + G\,K)^{-1}$ is the sensitivity function, K denotes the controller and G the plant model. The basic idea of mixed sensitivity design is to minimize the induced $\mathcal{L}_2$-norm of weighted closed-loop transfer functions by stacking them together.

There is a variety of weighting schemes in use, each with certain properties. It is however important to recognize that all mixed sensitivity approaches rely on the same principle: to shape the sensitivity function while achieving closed-loop stability. Every weighting scheme is thus in principle capable of achieving the same performance. This is due to the fact that the only degree of freedom in the minimization is the feedback controller K, on which all closed-loop transfer functions depend. This fact is sometimes mistaken in the mixed sensitivity approach and

is easier to recognize in an open loop shaping procedure, cf. Skogestad and Postlethwaite (2005).

Remark: For LPV systems, the notion of a transfer function does not exist. Still a "frozen parameter" interpretation is useful, especially in conjunction with the gridding approach that treats the LPV system as a family of LTI systems.

4.1 S/KS Design

Arguably, the most common weighting scheme is the S/KS scheme, i.e., $W_3 = I$. It seeks to directly shape the sensitivity function while limiting the control sensitivity. This makes it a very transparent weighting scheme: the sensitivity function is the primary indicator for performance and the control sensitivity restricts control authority and indicates robustness to unstructured additive (high frequency) perturbations such as unmodeled actuator dynamics.

The weighting filters for the design in this paper are selected to be diagonal, with W_1 consisting of one integrator per channel, whose crossover frequency determines the closed-loop bandwidth. The filter W_2 is also chosen diagonal, but with first order high-pass characteristics to enforce a roll-off in the controller. The S/KS scheme thus results in 4 filter states. Magnitude plots of the filters are given in Fig. 4.

4.2 Model Matching Design

Another frequently encountered approach is model matching, where $W_3 = T_{\text{ref}}$ is selected according to the desired closed-loop transfer function. The idea of imposing the dynamic properties of an ideal reference system on a closed-loop system has a long history in control engineering, see e.g. Limebeer et al. (1993). It seemingly provides an intuitive method to address transients, which is generally difficult in frequency-domain-based controller synthesis. With $W_3 = T_{\text{ref}}$, it follows from (9) that the minimization objective becomes

$$\min_K \left\| \begin{bmatrix} W_1\,S\,T_{\text{ref}} \\ W_2\,K\,S\,T_{\text{ref}} \end{bmatrix} \right\| = \min_K \left\| \begin{bmatrix} W_1\,(T\,T_{\text{ref}} - T_{\text{ref}}) \\ W_2\,(K\,S\,T_{\text{ref}}) \end{bmatrix} \right\| , \quad (10)$$

where $T = I - S$ is the complementary sensitivity function.

It is important at this point to note that the design inherently leads to a two-degree-of-freedom controller, i.e., while all closed-loop transfer functions maintain their interpretation, reference following is not anymore governed by the complementary sensitivity T alone. Instead, the transfer function for reference tracking becomes $T\,T_{\text{ref}}$. The minimization (10) thus seeks to minimize the difference between this reference transmission and the desired transfer function T_{ref}.

The natural choice of weighting filters resulting from this interpretation is to select T_{ref} with low-pass characteristics and unit steady state gain, W_1 as an integral weight to ensure model matching in steady state and a high-pass filter W_2 to limit control action due to changes in the reference signal. A problem with this choice is that the control sensitivity KS is also weighted with the low-pass filter T_{ref}, which contradicts classical design guidelines.
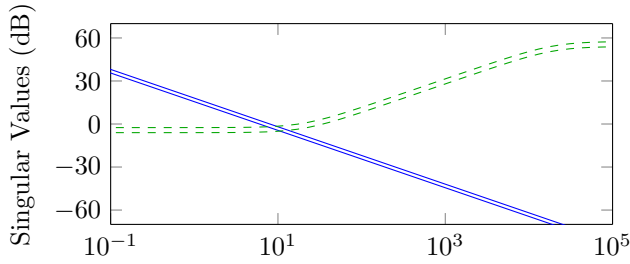
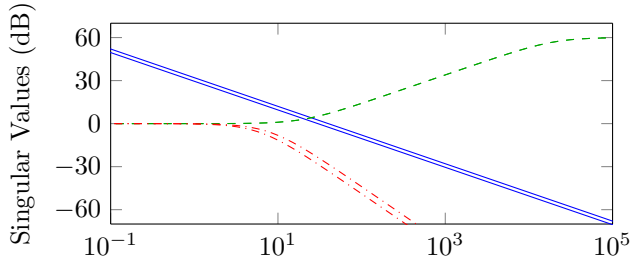Fig. 4. Weighting filters for S/KS scheme: W_1 (——) and W_2 (- - -)

Fig. 5. Weighting filters for model matching scheme: W_1 (——), W_2 (- - -) and W_3 (-·-·-)

This may lead to undesirably large control action in response to output disturbances and may significantly reduce robustness. In exchange, tuning is very simple with this scheme.

In accordance with the relative degree of the plant, a second order system with critical damping is selected as the reference model for each channel, i.e., T_{ref} is diagonal. A diagonal integral weight W_1 with a crossover frequency half a decade above the bandwidth of the reference model is used to assure model matching in a sufficiently large frequency range. Again, W_2 is selected as a diagonal first order high-pass filter. This eventually leads to a total number of 8 filter states for the model matching design. The corresponding magnitude plots are shown in Fig. 5.

5. EXPERIMENTAL RESULTS

In order to sufficiently cover the dynamic effects described in Section 2.2, it is necessary to include both negative and positive values for the angles q_2 and q_3 in the grid. Mirroring a positive grid still produced a stabilizing controller but with significant performance deterioration. An equally spaced grid of $3 \times 3 \times 7$ points is thus used to cover the operating range $\dot{q}_1 \in [30\,\frac{\text{rad}}{\text{s}}, 60\,\frac{\text{rad}}{\text{s}}]$, $q_2 \in [-25°, 25°]$, $q_3 \in [-75°, 75°]$. The rate bounds are selected as $|\ddot{q}_1| < 10\,\frac{\text{rad}}{\text{s}^2}$, $|\dot{q}_2| < 2\,\frac{\text{rad}}{\text{s}}$ and $|\dot{q}_3| < 2\,\frac{\text{rad}}{\text{s}}$ based on experimental observations.

An affine parameter-dependent Lyapunov matrix is selected for simplicity and the scheduling signals are normalized with respect to their maximum values, i.e.,

$$R(p) = R_0 + R_1 \frac{\dot{q}_1 - 30\,\frac{\text{rad}}{\text{s}^2}}{30\,\frac{\text{rad}}{\text{s}^2}} + R_2 \frac{q_2}{25°} + R_3 \frac{q_3}{75°} \,. \quad (11)$$

It is verified by using a lower bound on the achievable performance (see Saupe (2013)), that higher order basis functions do not significantly improve the result.
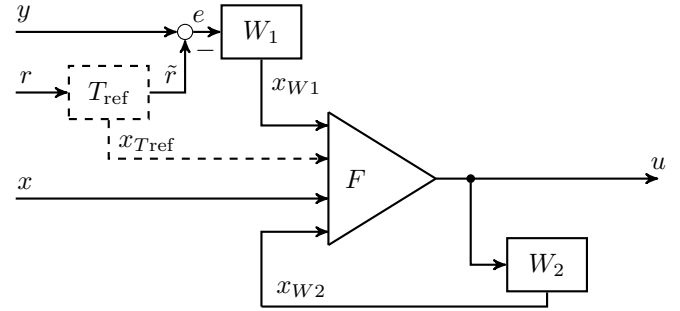

Fig. 6. Augmented state feedback controller with dashed lines indicating parts only applicable to the model matching design; otherwise $r = \tilde{r}$.

SDPT3 (Toh et al. (1999)) is employed to solve the minimization problem (8) with YALMIP (Löfberg (2004)) used as a parser. A suboptimal algorithm, developed in Saupe (2013), is used to ensure that the Lyapunov matrix R is well conditioned since it is inverted in the controller reconstruction step (6).

The experimental setup allows direct measurement of all angles q by means of encoders. In order to obtain the angular velocities $\dot{q}$, first order differentiation filters $D(s) = \frac{60\,\pi\,s}{s+60\,\pi}$ are used. The controllers are implemented in Simulink and deployed on a real time target. The gain calculation

$$F(p) = -\left(B_2^T(p)\,R^{-1}(p) + C_{12}\right) \quad (12)$$

is performed online at a sampling rate of 1100 kHz with the inversion of R efficiently carried out by LDL^T factorization, exploiting positive definiteness of R. The structure of the augmented state feedback controllers is shown in Fig. 6. The controllers inherit the dynamic order of the weighting filters, i.e., 4 for the S/KS and 8 for the model matching design.

Prior to each experiment, the flywheel is brought to its initial velocity using a PI regulator. Authority is then switched at $t = 15\,\text{s}$ to the LPV controller.

5.1 Trajectory Tracking

Both controllers were manually tuned until satisfactory performance was achieved. For comparison, the responses reported in Abbas et al. (2014) are used. Their LPV state feedback design employs the S/KS scheme with constant weights and uses an additional first order prefilter with a bandwidth of $10\,\frac{\text{rad}}{\text{s}}$ on the reference signal and a second static prefilter to reduce the steady state error. It is therefore also a two-degree-of-freedom design.

All three evaluated controllers achieve a similar level of performance in terms of the speed-of-response (Fig. 7). Both S/KS and model matching controller yield responses that are almost identical. Compared to the design of Abbas et al. (2014), cross couplings are significantly reduced and almost nonexistent with the dynamic controllers. Tracking accuracy is also clearly improved due to integral control.

It is also observed that the dynamic controllers deliver consistent results regardless of the direction of the reference steps. The controller by Abbas et al. (2014) is faster for steps towards the origin, while it is slightly slower in the opposite direction.
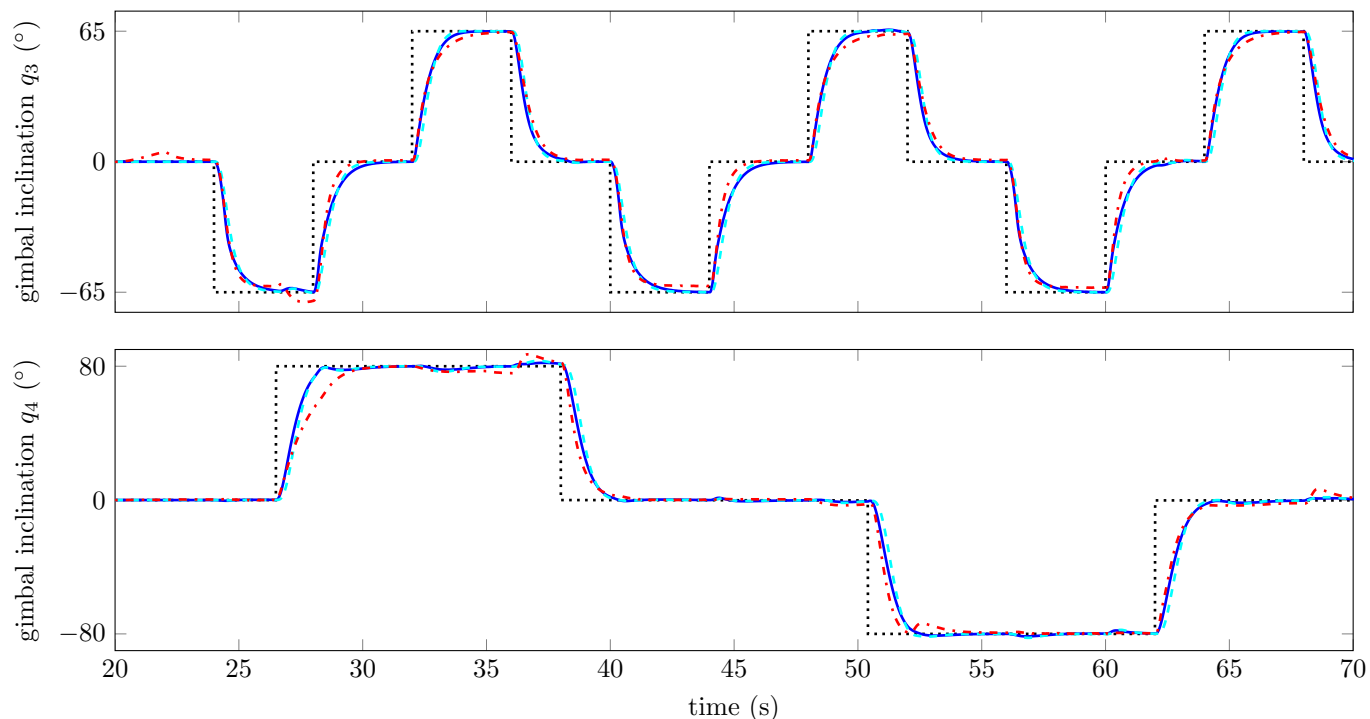
Fig. 7. Tracking of gimbal inclination q_3: reference ($\cdots\cdots$), controller by Abbas et al. (2014) ($\cdot$-$\cdot$-$\cdot$), S/KS (——) and model matching (- - -) controller
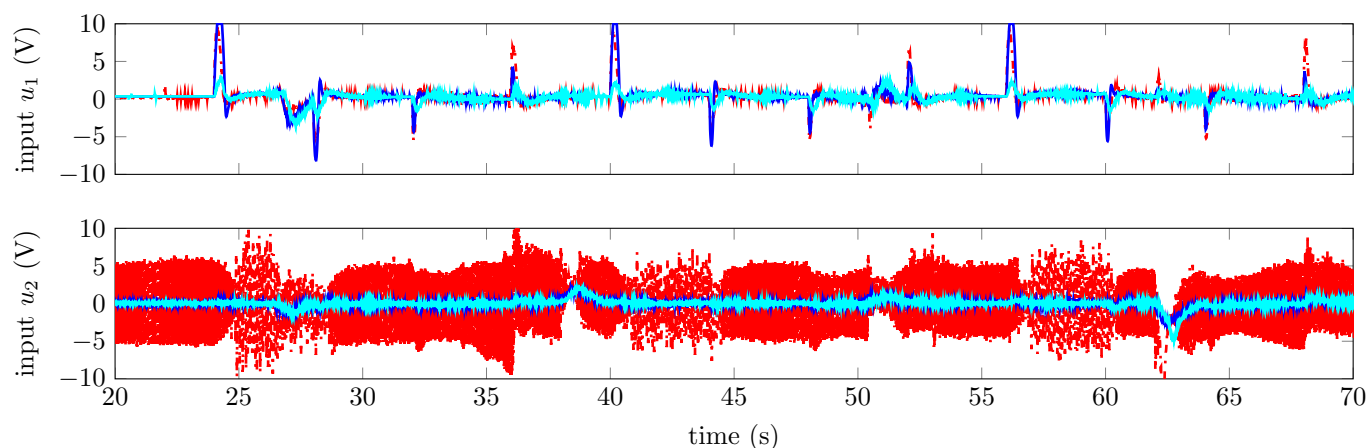
Fig. 8. Control input signal u saturated at ±10V: controller by Abbas et al. (2014) ($\cdot$-$\cdot$-$\cdot$), S/KS (——) and model matching (- - -) controller
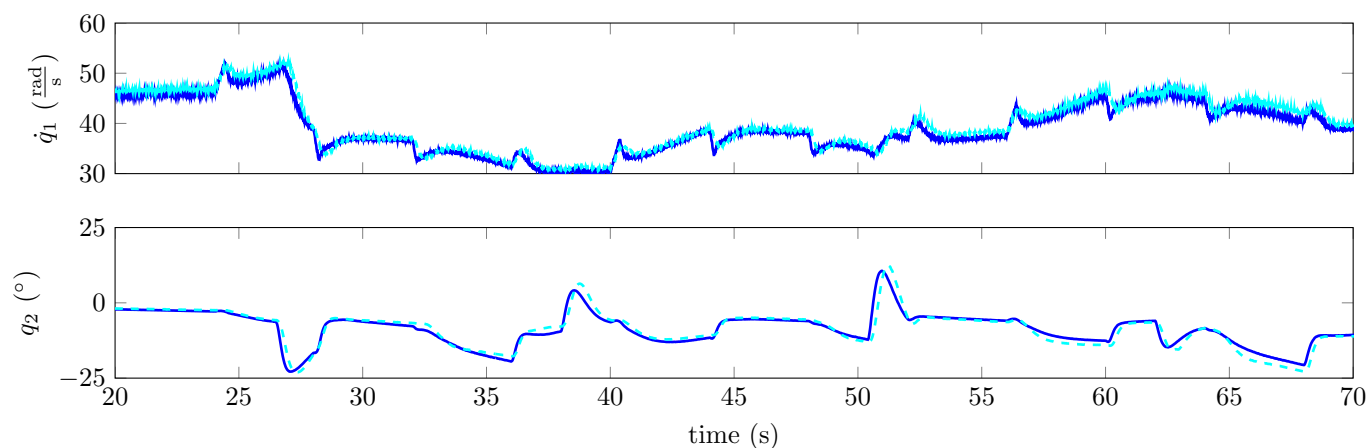

Fig. 9. Scheduling signals $\dot{q}_1$ and q_2 with S/KS (——) and model matching (- - -) controller
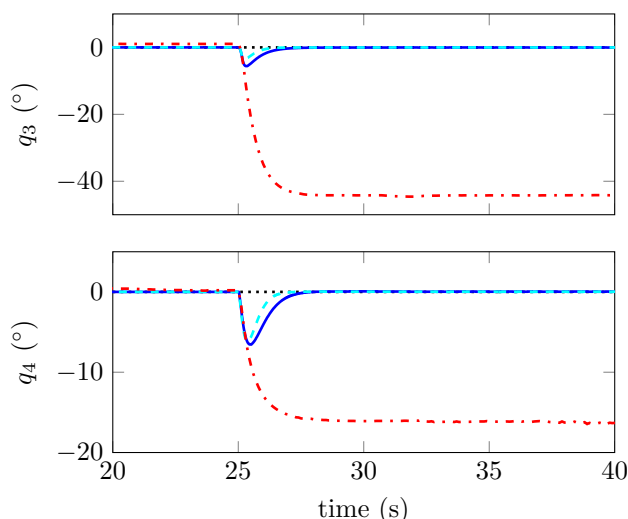
Fig. 10. Input disturbance rejection: reference (······), controller by Abbas et al. (2014) (·-·-·), S/KS (——) and model matching (‐ ‐ ‐) controller

A close examination further shows that the model matching controller produces responses with higher order characteristics, i.e., fast rise time with visible phase lag compared to the S/KS controller. This is expected from the additional prefiltering of the reference signal through T_{ref}.

The corresponding input signals are shown in Fig. 8. Input u_1 is very similar for all three controllers, with the model matching controller resulting in smaller peaks for changes in q_3 due to the prefiltered reference signal. Input u_2 is also very similar for S/KS and model matching controller but differs greatly from the controller by Abbas et al. (2014) that lacks a roll-off and thus amplifies measurement noise.

Fig. 9 shows the scheduling signal trajectories for S/KS and model matching controller. They can be verified to remain within the predefined bounds. The great resemblance of both trajectories further suggests good repeatability of the experiment since not only the controlled outputs but also the internal variables evolve similarly.

5.2 Input Disturbance Rejection

As a second experiment, an input disturbance is considered. A zero reference is provided and at $t = 25$ s, a step disturbance of 10 V is applied to each of the two input channels. The insufficiency of a static design for this scenario becomes readily apparent from Fig 10: while the static controller maintains a steady state offset of approximately 45° for q_3 and 16° for q_4, both dynamic controllers completely reject the disturbance. The S/KS controller results in a peak of 6° for both q_3 and q_4, and after 3 s, the input disturbance is compensated. The model matching controller achieves even slightly better results, with a peak of 4° for q_3, 6° for q_4 and 2 s until complete compensation. This is a consequence of the selected two-degree-of-freedom structure, in which the closed-loop bandwidth for disturbance rejection is larger than for reference tracking.

5.3 Conclusions

The experiments demonstrate the advantages to be gained by using augmented over static state feedback: the control effort is reduced through the use of a dynamic weight W_2 and steady state accuracy is guaranteed through integral control via W_1. This holds true even with input disturbances acting on the plant. Both, the S/KS and model matching approach achieve almost identical performance, where it should be recalled that the model matching controller is a two-degree-of-freedom design with twice as many dynamic states as the single-degree-of-freedom S/KS controller.

ACKNOWLEDGEMENTS

REFERENCES

Abbas, H., Ali, A., Hashemi, S., and Werner, H. (2013). LPV gain-scheduled control of a control moment gyroscope. In *American Control Conference*, 6841–6846.

Abbas, H., Ali, A., Hashemi, S., and Werner, H. (2014). LPV state-feedback control of a control moment gyroscope. *Control Engineering Practice*, 24, 129–137.

Kurz, T., Eberhard, P., Henninger, C., and Schiehlen, W. (2010). From Neweul to Neweul-M²: Symbolical equations of motion for multibody system analysis and synthesis. *Multibody System Dynamics*, 24(1), 25–41.

Limebeer, D.J.N., Kasenally, E.M., and Perkins, J.D. (1993). On the design of robust and two degree of freedom controllers. *Automatica*, 29(1), 157–168.

Löfberg, J. (2004). YALMIP : A toolbox for modeling and optimization in MATLAB. In *Proc. CACSD Conference*. Taipei, Taiwan. URL http://users.isy.liu.se/johanl/yalmip.

Rugh, W.J. and Shamma, J.S. (2000). Research on gain scheduling. *Automatica*, 36, 1401–1425.

Saupe, F. (2013). *Linear Parameter Varying Control Design for Industrial Manipulators*. Number 1223 in Fortschrittberichte VDI Reihe 8. VDI Verlag, Düsseldorf, Germany. ISBN 978-3-18-522308-2.

Skogestad, S. and Postlethwaite, I. (2005). *Multivariable Feedback Control*. Prentice Hall, Upper Saddle River, NJ, 2nd edition.

Toh, K., Tuetuencue, R., and Todd, M. (1999). SDPT3—a MATLAB software package for semidefinite programming. *Optimization Methods and Software*, 11, 545–581. URL www.math.nus.edu.sg/~mattohkc/sdpt3.html.

Wu, F. (1995). *Control of Linear Parameter Varying Systems*. Ph.D. thesis, Univ. California, Berkeley.

Wu, F., Yang, X., Packard, A., and Becker, G. (1996). Induced $\mathcal{L}_2$-norm control for LPV systems with bounded parameter variation rates. *Int. J. Robust Nonlinear Control*, 6, 2379–2383.

Zhou, K., Doyle, J.C., and Glover, K. (1995). *Robust and Optimal Control*. Prentice Hall, Upper Saddle River, NJ.